Polymer Degradation and Stability 242 (2025) 111631

Contents lists available at ScienceDirect

Polymer Degradation and Stability

journal homepage: www.journals.elsevier.com/polymer-degradation-and-stability

Mechanistic study of enzymatic hydrolysis of poly(butylene succinate)/poly (pentamethylene 2,5-furanoate)-based blend and block copolymer

Chiara Siracusa [a,b], Mattia Manfroni [c], Alessandro Coatti [c], Felice Quartinello [a], Michelina Soccio [c,d,e,*], Nadia Lotti [c,d,f], Georg M. Guebitz [a,b], Alessandro Pellis [a,b,g,*]

[a] acib GmbH, Konrad-Lorenz-Strasse 20, 3430 Tulln an der Donau, Austria
[b] Institute of Environmental Biotechnology, Department of Agrobiotechnology, IFA-Tulln, BOKU-University, Vienna Konrad-Lorenz-Strasse 20, 3430 Tulln an der Donau, Austria
[c] Department of Civil, Chemical, Environmental and Materials Engineering, University of Bologna, Via Terracini 28, Bologna, 40131, Italy
[d] Interdepartmental Center for Industrial Research on Advanced Applications in Mechanical Engineering and Materials Technology, CIRI-MAM, Viale del Risorgimento 2, 40136, Bologna, Italy
[e] Interdepartmental Center for Industrial Research on Buildings and Construction CIRI-EC, Via del Lazzaretto 15/5, 40131, Bologna, Italy
[f] Interdepartmental Center for Industrial Agro-Food Research, CIRI-AGRO, Via Quinto Bucci 336, 47521, Cesena Italy
[g] Department of Chemistry and Industrial Chemistry, Università degli Studi di Genova, Via Dodecaneso 31, 16146 Genova, Italy

ARTICLE INFO

Keywords:
Biobased plastics
Sustainable packaging
Enzymatic recycling
Poly(butylene succinate)
Furan-based materials
Enzymatic depolymerization

ABSTRACT

Poly(butylene succinate)(PBS) and poly(pentamethylene 2,5-furanoate)(PPeF) are bio-based polymers that proved to be compatible to derive versatile blends. The different mechanical properties resulting from their combinations respond to the diverse needs in food packaging. While already their physical blending lead to products with good flexibility, copolymers showed further improved elasticity while maintaining good gas barrier properties. The possibility of being fully degraded through hydrolytic enzymes places an additional advantage to the fully green potential of these polymers. The two homopolymers, their physical blend as well as copolymer were demonstrated to be decomposed by the *Humicola insolens* cutinase (HiC) reaching 100 % of weight loss after 24 h of incubation. PBS was hydrolysed faster than PPeF, while, interestingly, at 50 % content of each polymer, the physical blend was more susceptible to enzymatic hydrolysis than the copolymer, as resulted from weight loss and HPLC quantification of the released monomers. This trend was even more pronounced related to reduction of molecular weight during the first phase of hydrolysis as indicated by Gel Permeation Chromatography analysis. Surface characterization of the polymers during hydrolysis by using Fourier Transform Infrared Spectroscopy likewise confirmed faster hydrolysis of PBS moieties. Nuclear Magnetic Resonance highlighted slower appearance of hydrolysis-related groups in the copolymer when compared to the physical blend. Overall, this mechanistic study indicates that blending or synthetizing copolymers can influence enzymatic hydrolysis with important implications towards exploitation of enzymes as an environmentally benign emerging technology for recycling.

1. Introduction

The amount of waste generated from packaging is escalating. Almost 190 kg of packaging waste pro capita were generated in Europe in 2021, which corresponds to an increase of 32 kg per person over 10 years. This value is expected to further increase to 209 kg in 2030 if no countermeasures are put into place. Approximately 20 % of the packaging waste amount is plastic and thanks to a stringent control in the last decade, the recycling rate has increased in parallel with waste generation [1]. Nevertheless, the recycling rate has plateaued at around 40 % according to the last years statistics. In fact, despite the campaign in favour of reducing plastics employment, plastic packaging is indispensable in all sectors, especially for food and hygiene items [2]. Moreover, the heterogenicity of the plastic management across EU countries justifies the intervention for common packaging design and recycling strategies for an environmentally respectful approach without colliding with final

* Corresponding authors.
E-mail addresses: m.soccio@unibo.it (M. Soccio), alessandro.pellis@unige.it (A. Pellis).

https://doi.org/10.1016/j.polymdegradstab.2025.111631
Received 25 July 2025; Received in revised form 26 August 2025; Accepted 27 August 2025
Available online 29 August 2025

product functionality and consumer safety. The aim is to prevent valuable materials and energy from exiting the production chain through high quality recycling, at the same time bypassing fossil sources [3].

This necessity has been translated into the research of alternative materials. Currently, poly(propylene) (PP), poly(ethylene) (PE) and poly (ethylene terephthalate) (PET) are the most common plastics. Their production mainly relies on fossil sources. For example, PET is derived from a fossil-based monomer: terephthalic acid (TPA). A possible substitute for TPA has been identified with 2,5-furandicarboxylic acid (FDCA), which is now obtained on a large scale from renewable raw materials [4]. This has led to the formulation of a growing class of polymers, which employs combinations of FDCA with different diols varying in chain length [5–8]. They proved to be excellent in terms of gas barrier and mechanical properties, as well as degradability [9], claiming the title of next generation polyester [10]. Therefore, the introduction of these products, with PEF as the bio-based counterpart [11] of PET, has been gradually implemented in the packaging market, where the largest share among the biobased plastics consists of poly (lactic acid) [12].

Poly(butylene succinate) (PBS) is another major player in biodegradable food packaging sector, extensively characterized from the mechanical and chemical point of view [13]. Showa Denko (Japan) was the first company to launch PBS as plastic on the market in the 1990s and passed the baton to Mitsubishi Chemical Corporation (Japan) in the early 2000s. While its production was already at an industrial scale, but unfortunately based on fossils [14], a shift towards biological sources was boosted during the recent years, leading to a 20 % decreased environmental impact. Corn, sugar cane and sugar beet, as well as lignocellulose and other biological materials, were identified as candidates to obtain succinic acid and butanediol, the PBS building blocks, in a fully biobased workflow [15]. Nevertheless, upgrades are necessary to reduce competition with food production. For this reason, not only were non-edible by-products of food and non-food crops introduced as sources for raw materials, but also innovative technologies such as enzymatic hydrolysis have been investigated to manage a green recycling of the after-use products [16].

PBS has been made available as neat homopolymer, but also as copolyester, or blended with aromatic polymers or organic materials for the realization of ionomers or nanocomposites, to improve the versatility and the final properties of the material [14]. A well-known example has been the combination with PBAT, which successfully merged PBS synthetic easiness with PBAT mechanical properties [17].

Due to the biobased origin and well-known better biodegradability of PEF compared to TPA-based polyesters though, furans have been replacing the latter also in copolymeric/blend formulations. Newly designed representatives of the class were also successfully combined with PBS, offering a fully biologically derived polymer [18]. In the present work, new biopolymers derived from physical blending as well as copolymerization of PBS with a furan-based polyester, poly(pentamethylene 2,5-furandicarboxylate) (PPeF) [19], have been subjected to biodegradation studies. PPeF presents really outstanding gas barrier ability and mechanical response recalling an elastomer [20].

The more complex manufacturing, together with possible food residue contamination, implies challenges in recycling, leading to direct disposal and subsequent accumulation in landfills [13]. The introduction of additives or other polymer components can alter the whole product degradability in biological context, because of the potentially different response of each component to biodegradation. This explains the interest to unravel mechanisms of depolymerization, which would allow the specific enzymatic recovery of valuable polymer building blocks e.g. from mixed waste.

Indeed, PBS depolymerization by enzymes has been already investigated in the last years, but mainly to explore the biomedical potential of these polymers [14]. In 2015, 15 % weight loss in 60 h of incubation has been reported through *Burkholderia cepacia* [21]. Other cutinases were applied to achieve significant surface erosion, while lypozyme CaLB preferentially mediates a bulk erosion.

Some studies of biodegradation are reviewed by Raza Miah et al. [10], but report mainly the behaviour of the FDCA-based polymers in a simulation of natural polyester biodegradation, where this process is investigated in its dependence on hydrophilicity, temperature, crystallinity, chemical structure, morphology and molecular weight. Enzymatic depolymerization was already employed for PEF degradation assessment [22] and PPeF [23], but deeper investigation of the enzymatic hydrolysis is still needed [24], especially within the view of food packaging application. This was achieved while investigating how the materials combine and blend, observing the process in a controlled environment. These insights would be then necessary to tune blend properties and improve its design in a combinatorial approach. In particular, the adoption of whole sample NMR and GPC to gain insights about the molecular mechanisms of hydrolysis, is fundamental to differentiate the aromatic from the aliphatic domains with respect to the depolymerization process of the respective blend/copolymer components [25].

Depolymerization of these materials was achieved with good yield, while at the same time, the monomer can be recovered with high purity [23]. The enzymatic treatment offers a customized approach with different outcomes/possibilities depending on the starting condition of the waste. The reaction can be tuned to reach a compromise between degradability, full depolymerization and at refining of the amount of enzyme applied. Reducing the rate and modulating the reaction also opens windows to observe how the recycling process occurs and can be optimized, as well as how this can be adopted for functionalization purposes.

2. Materials

2.1. Chemicals and substrates

Poly(1,4-butylene succinate) (PBS) and poly(1,5-pentamethylene 2,5-furanoate) (PPeF) homopolymers, and their equiponderal physical blend (PBS/PPeF) and block copolymer ($P(BS\text{-}b\text{-}PeF)_{15}$) were prepared as reported in the following. Di-Potassium hydrogen phosphate (K_2HPO_4) for buffer preparation was provided by Roth (Germany). Other chemicals and pure monomers (2,5-furandicarboxylic acid, 1,4-butanediol, succinic acid, 1,5-pentanediol) for instrument calibration and purity comparison were purchased by Sigma-Aldrich. The commercially available enzyme *Humicola insolens* cutinase (hereby abbreviated as HiC) is a product from Novozymes.

2.2. Methods

2.2.1. Synthesis of homopolyesters

Poly(butylene succinate) (PBS) and poly(pentamethylene 2,5-furanoate) (PPeF) were prepared by a bulk two-step polycondensation process. The reaction was conducted in a 250 mL thermostatted stirred glass reactor. For PBS homopolymer, the reactor was charged with dimethyl succinate and 1,4-butanediol in a 1:1.2 molar ratio, respectively, together with titanium tetrabutoxide as catalyst (400 ppm). The first step was carried out in an inert N_2 atmosphere and continuous stirring (50 rpm) at 190 °C. During this first stage, transesterification took place with the release of methanol which was removed from the reaction mixture by distillation and collected in a glass trap downstream of the reactor. Transesterification was considered completed once 90 % of theoretical MeOH was collected, i.e. after 90 min. In the second polycondensation step, the reacting system was gradually heated to 220 °C and the pressure was simultaneously reduced to 0.05 mbar. The second stage was concluded after 3.5 h, once a constant torque value was measured. Finally, the polymer was easily discharged from the reactor and stored at room temperature. PPeF was prepared following the same procedure used for PBS: in a 250 mL thermostatted stirred glass reactor dimethyl furan-2,5-dicarboxylate, 1,5-pentanediol were charged in a

1:1.5 molar ratio, along with the catalysts (titanium tetrabutoxide 200 ppm and titanium isopropoxide 200 ppm). The first and second step times were 90 min and 3.0 h, respectively (Scheme 1, previous work [19]).

2.2.2. Blend preparation

PBS and PPeF were dissolved in chloroform (50/50 wt/wt). The resulting solution was cast onto a Petri dish, and the solvent was let evaporate. Solution mixing and casting ensured the obtainment of a physical blend, avoiding transesterification reactions between PBS and PPeF, otherwise favored by high temperatures during melt mixing (Scheme 1, previous work [19]). The equiponderal physical blend referred to as PBS/PPeF.

2.2.3. Synthesis of block copolymer

Block copolymers were synthesized starting from PBS/PPeF physical mixture through reactive blending carried out in bulk, under stirring at 220 °C for 15 min, employing a glass reactor under a nitrogen atmosphere. The sample is designated as P(BS-*b*-PeF)$_{15}$ where 15 represents the mixing time (Scheme 1, previous work [19]).

2.2.4. Film preparation

Polymeric films with an average thickness of 150 μm were prepared by compression molding using a laboratory press Carver C12. The as-synthesized homopolymers and block copolymer, as well as the physical blend, were put into two Teflon sheets and heated at 40 °C above the relative melting temperature (or glass transition temperature in case of amorphous PPeF). Once molten, a pressure of 8 tons m^{-2} was applied for 2 min. Finally, films were cooled down (through water cooling coils) to room temperature and stored for 10 days before further characterization to attain the equilibrium crystallinity.

2.2.5. Molecular and thermal characterization

NMR spectroscopy (Varian XL-400 NMR spectrometer (Palo Alto, CA, USA)) was used for the determination of chemical structure, composition and randomness degree. Molecular weights were determined by gel-permeation chromatography (GPC) at 30 °C using an HPLC Lab Flow 2000 apparatus (KNAUER, Berlin, Germany), using chloroform as the mobile phase and monodisperse polystyrene standards for the calibration curve.

DSC analysis was employed to determine the main thermal transitions in the polymer samples (Pyris DSC6 calorimeter (PerkinElmer, Shelton, CT, USA)). Glass transition temperature (T_g) was calculated as the midpoint of the glass-to-rubber transition step. Melting temperature (T_m) and the corresponding were taken from the peak maximum and total area, respectively.

Scheme 1 shows the overall path of the synthesis of PBS and PPeF homopolymers, physical blend and block copolymer. In Table 1 the main molecular and thermal data for PBS, PPeF, PBS/PPeF and P(BS-*b*-PeF)$_{15}$ films [19] are summarized. All the polymers show high molecular weight. PBS/PPeF is the mere sum of neat homopolymer, while P(BS-*b*-PeF)$_{15}$, as a consequence of the shortening of butylene succinate (BS) segments and to the presence of pentamethylene furanoate (PeF) units, presents lower melting temperature and enthalpy with respect to PBS homopolymer.

2.2.6. Enzyme and sample preparation for hydrolysis

Protein concentration and enzyme activity were measured through spectrophotometry. The Bradford protein assay was performed to calculate the total protein content of the solution after the comparison with a standard curve previously determined with Bovine Serum Albumin (BSA) as a reference. The enzyme activity on the model substrate *para*-nitrophenylbutyrate (*p*-NPB) was measured by monitoring the increase of the *para*-nitrophenolate ion resulting from the hydrolysis of the substrate at 405 nm. Each value was compared to water absorbance as a blank. Tecan Plate Reader (Tecan, Grödig, Austria, Infinite M200 PRO) was used to measure at the respective wavelength.

The homopolymers, copolymer and physical blend specimens were equally sized to 1 × 0.5 cm^2 and cleaned from impurities as previously described [22]. The initial weight of each dried sample was determined, before placing them in 2 mL Eppendorf tubes where the incubation was performed. Potassium phosphate buffer (1 M, pH 8) was added to the control reactions. HiC was supplemented in the same buffer to three different final concentrations: 1 μM, 2.5 μM or 5 μM. The tubes were placed horizontally in an orbital shaker incubator at 65 °C and 150 rpm agitation. Samples were collected after 3, 6, 9, and 24 h for all the polymers. Additionally, 5 μM HiC reaction was monitored until 48 h and 72 h. Control and enzymatic incubations were performed in triplicate per each time point.

After sampling, each Eppendorf tube was cooled down to 4 °C. One sample of each triplicate was lyophilized for whole sample NMR characterization. The rest was separated in the hydrolysate fraction and residual films for respectively monomer concentration determination and weight/surface analysis.

2.2.7. Weight loss and surface characterization of partially degraded samples (FT-IR and SEM)

Polyester residual fragments after hydrolysis were isolated and washed according to the same preparation protocol. The weight loss was determined comparing the final weight (mg) to the original one (mg) and expressed in percentage. PerkinElmer Spectrum 100 Spectrometer in ATR mode was used for the detection of the surface functional group characterization through Fourier Transform Infrared Spectroscopy (FT-IR). All spectra were collected for 40 scans, between 4000 and 650 cm^{-1} wavelengths, with a resolution of 2 cm^{-1}. The software PerkinElmer data manager (Spectrum Programme version: 10.01.00.0030) was used to acquire and process the spectra. Surface morphology was additionally imaged through Scanning Electron Microscopy (SEM), using a Hitachi

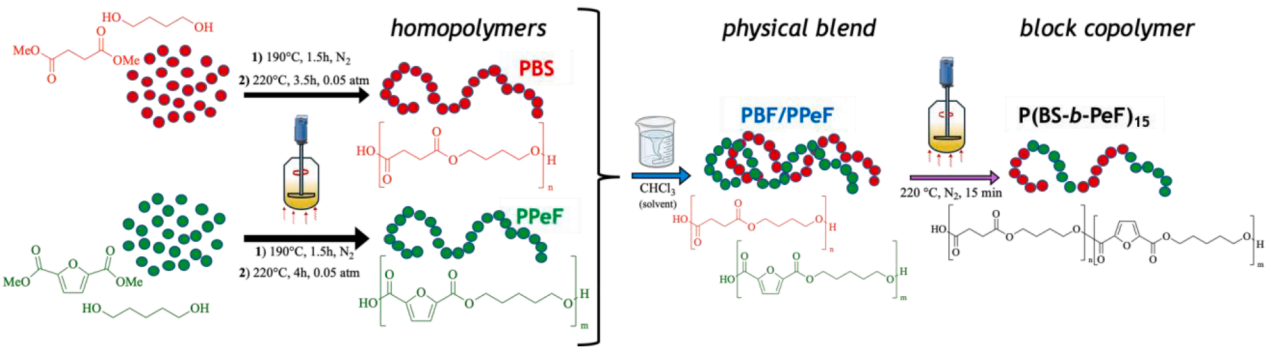

Scheme 1. Schematic representation of: PBS and PPeF syntheses, PBS/PPeF physical blend preparation and reactive blending to obtain the P(BS-*b*-PeF)$_{15}$ block copolymer [19].

Table 1
Molecular and thermal characterization data of PBS, PPeF and P(BS-*b*-PeF)$_{15}$ block copolymer. PBS/PPeF is the mere sum of neat homopolymers [19].

Sample	PBS wt %	M_n g/mol	D	BS $_{block\ length}$	PeF $_{block\ length}$	*Degree of randomness (b)*	T_g °C	T_m °C	ΔH_m J/g
PBS	100	49,100	2.1	≈280	—	—	−32	113	60
PBS/PPeF	50	–	–	≈280	≈170	0	12	113	34
P(BS-*b*-PeF)$_{15}$	50	43,200	2.1	10	8.5	0.2	−19	79	17
PPeF	0	37,800	2.2	—	≈170	—	17	–	–

3030TM Microscope (Metrohm INULA GmbH, Austria) to collect secondary electrons. Before picture acquisition, each sample was covered with 3 nm platinum layer through sputter coating device (Details).

2.2.8. Soluble released products quantification via HPLC

Ice cold methanol was added to each refrigerated sample (4 °C) to stop the enzymatic reaction and drive enzyme removal. HPLC vials for soluble monomer detection were prepared after acidification (30 μL 6 N HCl), centrifugation (14,000 rpm, 4 °C, 15 minutes) and filtration (0.2 μm polyamide filters). Vials were then analysed through High Performance Liquid Chromatography (HPLC) (Agilent Technologies, 1260 Infinity) supplied with a reversed phase column C18 and UV (260 nm) for FDCA detection or Refractive Index Detector (RI, Transgenomic ICSEP-ION-300) for linear compound detection (1,5-pentanediol, 1,4-butanediol, succinic acid). In the latter case, Carrez precipitation was performed before centrifugation and filtration into HPLC vials, as previously described [23]. The concentration of each monomer was then quantitatively estimated through comparison with the corresponding calibration curves.

2.2.9. Molecular characterization: gel permeation chromatography (GPC) and nuclear magnetic resonance (NMR)

Proton Nuclear Magnetic Resonance (^{1}H NMR) spectroscopy was performed after solubilization of one hydrolysate of each triplicate in deuterated $CHCl_3$ at room temperature. Tubes were then analysed through a JEOL ECZ400R/S3 instrument at a frequency of 400 MHz.

An additional replicate was solubilized in $CHCl_3$ to a final concentration of 2 mg mL^{-1}, then filtered through cotton in a Gas Permeation Chromatography (GPC) vial. Samples were run at 30 °C through a HPLC Lab Flow2000 instrument (KNAUER, Berlin, Germany) provided with a Rheodyne 7725i injector, Phenomenex MXL 5 μm mixed bed column, and a RI K-2301 KNAUER detector. The mobile phase used was chloroform at a fixed flow rate of 1.0 mL min^{-1}. Standards in use for the calibration curve were Monodisperse polystyrene standards (Sigma Aldrich Chemical Co., St. Louis, MO, USA). Results were then processed through Agilent GPC/SEC software.

3. Results and discussion

3.1. Enzymatic hydrolysis of PBS, PPEF and their physical blends and copolymers

The cutinase from *Humicola insolens* was chosen to mechanistically investigate the hydrolysis of equiponderal blend and block copolymer of PBS and PPeF as it was previously found to be active on blends and copolymer of PPeF with PLA [23]. The reaction was carried out at 65 °C since temperature alone favours the flexible rubbery state of the polymer matrix, especially because it was kept higher than the glass transition temperature of all the polymers (though lower than the melting point, 113 °C for the homopolymers and the physical blend and 79 °C for the block copolymer). After 24 h of incubation with the enzyme, a complete weight loss was recorded for all the polymers and at all tested enzyme concentrations (Figure S1, ESI), justifying a narrowing in the time point collection (within the first day: at 3 h, 6 h and 9 h) (Fig. 1).

Incubation of PBS and the physical blend with PPeF with 1 μM HiC lead to a complete weight loss already within the first 3 h. On the other hand, the PPeF homopolymer and P(BS-*b*-PeF)$_{15}$ copolymer were more recalcitrant to enzymatic hydrolysis and at the identical enzyme concentration complete weight loss was observed only after 24 h of incubation, differently from what was observed in PLA/PPeF blend [23], where PPeF was the preferentially cleaved component of the blend. A higher concentration of enzyme, namely 5 μM, lead to a PPeF weight loss ranging from 33 % (3 h) to 59 % (6 h) to 89 % (9 h) within the first day of incubation. Quite expectedly, the copolymer showed a faster weight loss: 1 μM HiC incubation resulted in a percentage of weight loss ranging from 63 %, to 73 % and to 90 % within the first 3 h, 6 h and 9 h of reaction, respectively. All together, these results indicate a preference of the enzyme to the aliphatic PBS when compared to aromatic PPeF. A first interesting hypothesis could be drawn about a faster hydrolysis of the physical blend compared to the copolymer, confirming previous experimental results [23]: keeping fixed the relative amounts (PBS 50 % and PPeF 50 %), the weight loss is slower when the more recalcitrant PPeF component is chemically linked to PBS. A possible explanation for the different degradation behaviour of the blend compared to the

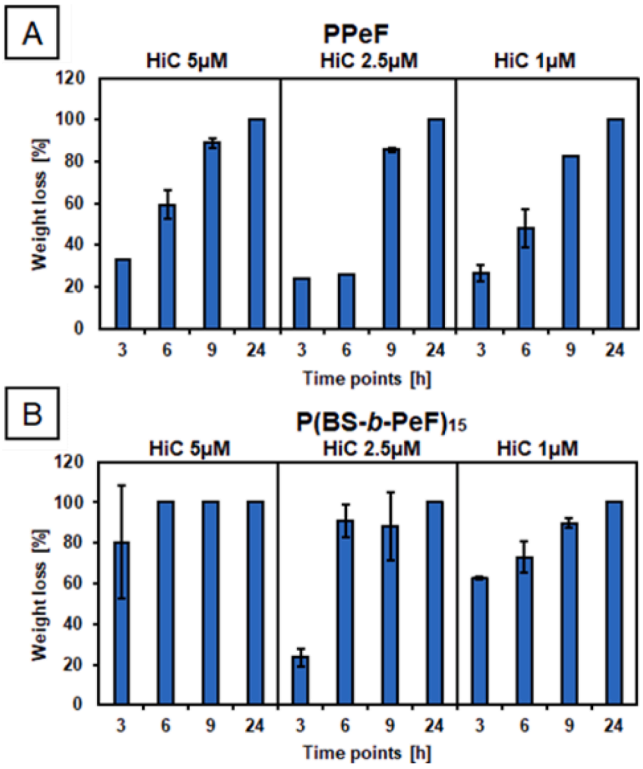

Fig. 1. Weight loss of PPeF and P(BS-b-PeF)$_{15}$ upon enzymatic hydrolysis. 1 × 0.5 cm films were incubated at 65 °C, and 150 rpm with different concentrations of the cutinase HiC, namely 1 μM, 2.5 μM and 5 μM. Histograms of each time point at 3 h, 6 h, 9 h, 24 h and controls at 24 h with standard deviation were calculated on triplicate samples. A: PPeF; B: P(BS-b-PeF)$_{15}$. No weight loss was seen in the respective control samples without enzyme while pure PBS and the physical blend were completely decomposed already after 3 h (see figure S1).

copolymer could lie in their phase differences. As reported by Manfroni et al. [19], an interface between the continuous matrix of PBS and the dispersed microdomains of PPeF is visible in the PBS/PPeF blends, but not in the copolymer. Such phase separation between PBS and PPeF would facilitate the accessibility of the degradative agents to the amorphous domains and interfacial regions, with overall promotion of ester bond hydrolysis. The copolymer would in fact have a more homogenous microstructure, where the polymer chains are packed and less mobile/accessible. This is also coupled with a slightly inferior crystallinity of the blended polymer, a key player in enzyme accessibility.

3.2. Release of soluble monomers

Upon incubation with 5 μM HiC, 58.84 mM FDCA were released from PPeF after 24 h (Fig. 2B). Likewise, release of the second building block of PPeF, namely 1,5-pentanediol (PDO), was seen. The ratio between the two building blocks was found to be dependent mostly on the incubation time and enzyme concentration. More in detail, FDCA/PDO ratio increased with incubation time and enzyme concentration. This indicated that the polymer forms in a first step oligomers, while in a second step preferentially FDCA is released from those. For PBS, lower enzyme concentration led to a higher amount of BDO indicating, in contrast to PPeF, that in a first phase preferentially the glycol and not the acid is released from intermediately formed oligomers, whereas at higher enzyme concentrations the ratio between the two building blocks established at 1:1 ratio. 2.5 μM HiC lead to a maximum release of monomers after 24 h of incubation without further increase at higher enzyme dosage (5 μM HiC). As for the lowest enzyme concentration, 1 μM HiC, the reaction lead to minor depolymerization than 5 μM or 2.5 μM in terms of absolute soluble monomers. Nevertheless, the depolymerization occurred and gradient of monomer release was steeper, which confirms the possibility of adopting these settings to study closer the mechanisms of hydrolysis. Overall, in contrast to the weight loss results, a slightly lower amount of released monomers was seen for PBS when compared to PPeF, which could be due to the formation of soluble oligomers. Nevertheless, higher amounts of PBS building blocks measured after incubation of both PBS/PPeF blend and P(BS-*b*-PeF)$_{15}$ copolymer clearly indicated preferential cleavage of aliphatic ester bonds by the enzyme. In agreement with the weight loss results, a higher activity was seen on the blend when compared to the P(BS-*b*-PeF)$_{15}$ copolymer.

3.3. Surface characterization via SEM and FT-IR

Through Scanning Electron Microscopy (SEM), it was possible to observe that PBS and PPeF were well compatible since the physical blend shows a homogenous surface (Figure S2) [24]. The incubated samples were not recovered, therefore only the copolymer was characterized in the different time points. The residual films were coated with 3 nm platinum layer, to increase the contrast and the difference in the matrix across the time course of incubation. Figure S3 shows the progressively larger and more diffused pores originating after longer incubation with the enzyme, also at low concentration. Similar results were seed for the intermediate HiC amount, which resulted in enlarged porous structure, especially visible at 1000X magnification (Figure S4). 5 μM HiC treated polymers could only be analysed after 3 h of incubation, due to a 100 % weight loss after longer times. These residual polymers showed already at the first time point the same macroscopic structure that the previously analysed ones (Figures S3–5) displayed after 9 h of incubation, confirming the proportionality between the amount of enzyme and the effect on the polymer hydrolysis. In particular, higher magnification (2500x) showed more closely the degradation patterns of each polymer surface, appeared at later time points when the incubation was performed with lower amount of enzyme (Fig. 3). The erosion patterns configurating as regions with lower densities could be ascribed to the polymer formulation, which was produced as a block

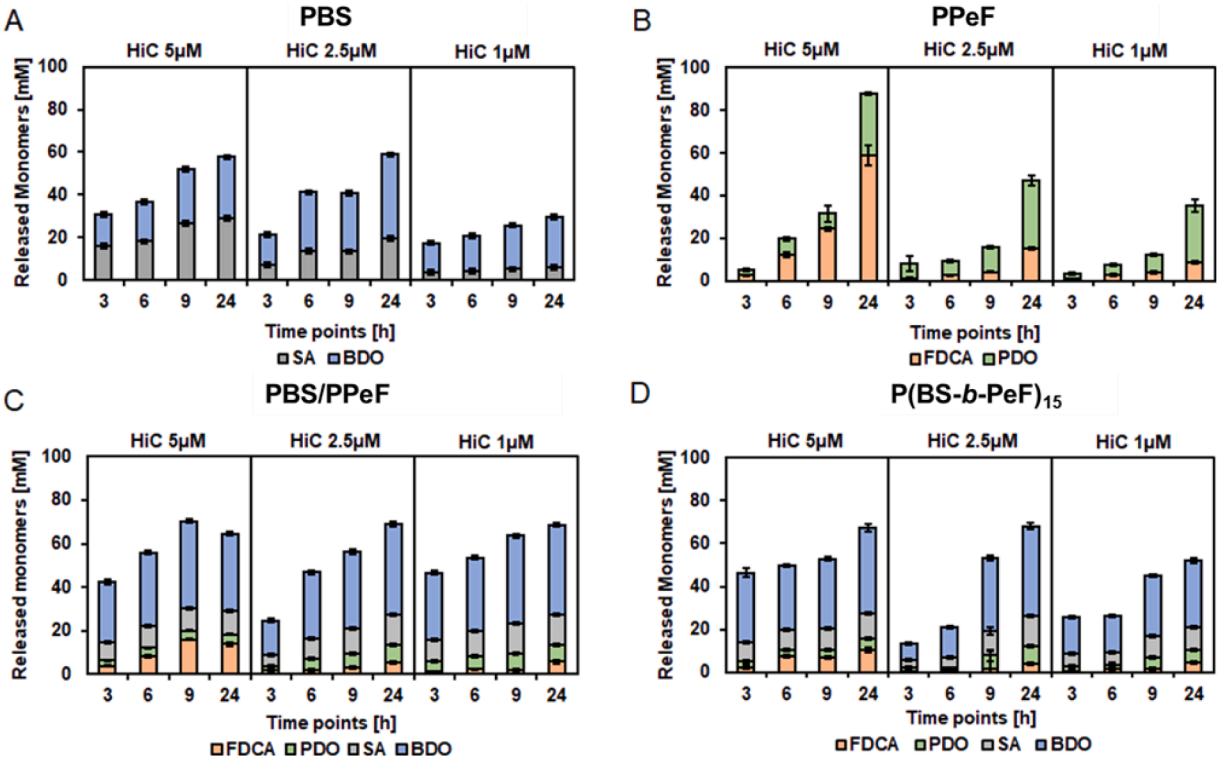

Fig. 2. HPLC-quantified released soluble monomers from 0.5 cm x 1.0 cm films incubated with 5 μM, 2.5 μM and 1 μM HiC. A: PBS, B: PPeF, C: PBS/PPeF, D: P(BS-*b*-PeF)$_{15}$. Orange bars: 2,5-furandicarboxylic acid (FDCA); green bars: pentanediol (PDO); grey bars: Succinic acid; blue bars: 1,4-butanediol (BDO). Histograms are average of triplicates. No monomers were detected in the control samples without enzyme.

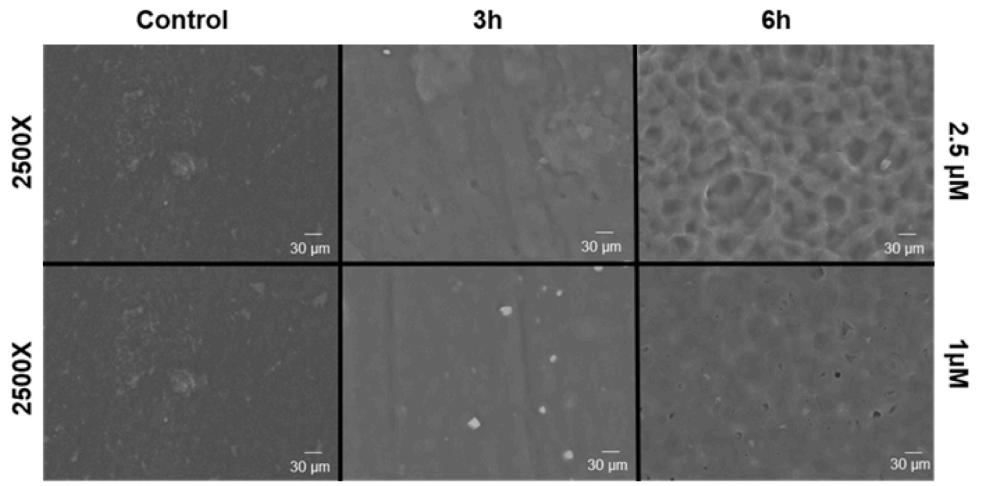

Fig. 3. SEM pictures of the residual block copolymer (P(BS-*b*-PeF)$_{15}$) at 2500x magnification after 3 h and 6 h of incubation, showing degradation patterns compared to the control sample.

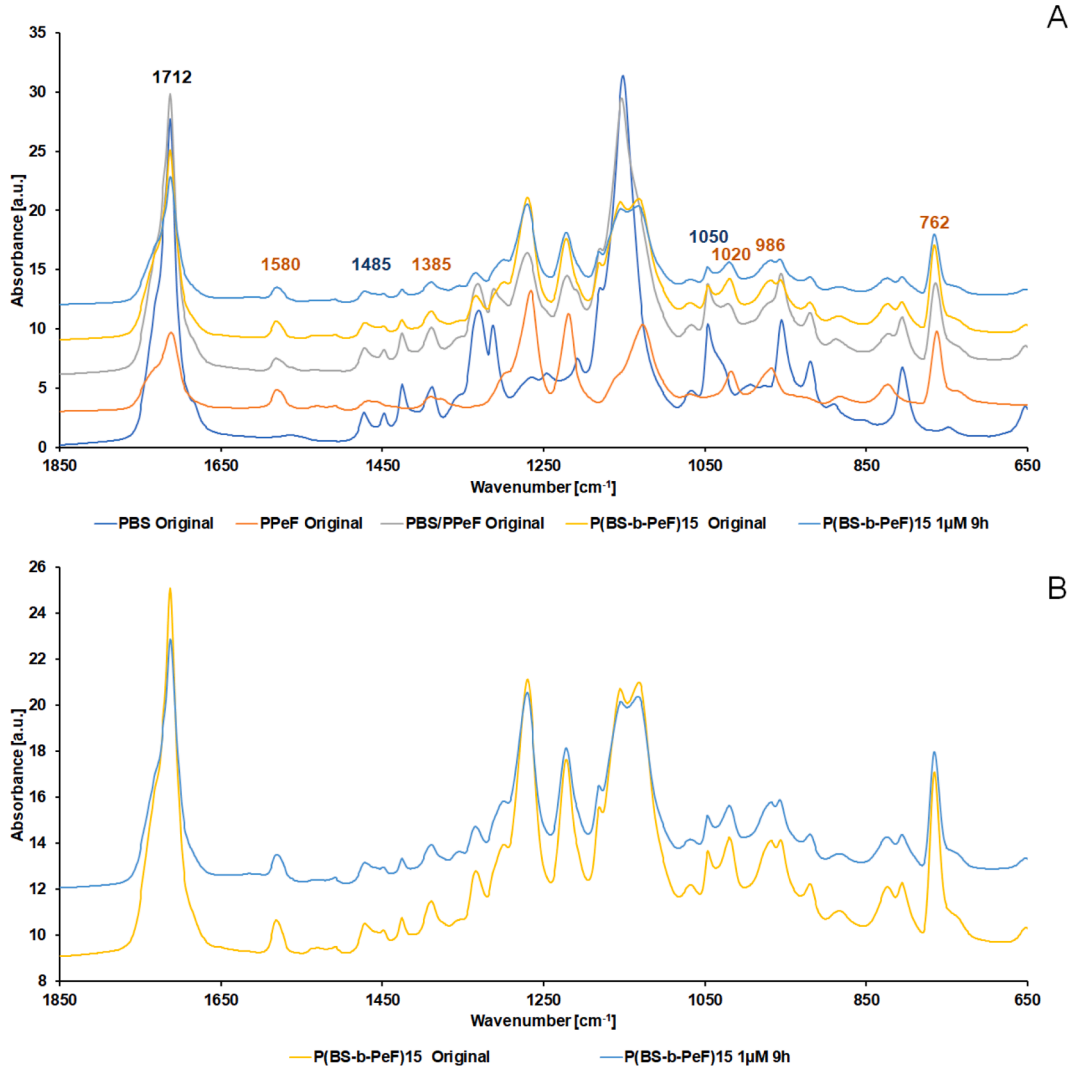

Fig. 4. A: FT-IR stacked spectra of PBS, PPeF, PBS/PPeF physical blend and P(BS-*b*-PeF)$_{15}$ copolymer compared to the last recoverable sample from P(BS-*b*-PeF)$_{15}$ hydrolysis with a zoom in the range 1850 cm^{-1} – 650 cm^{-1}. From bottom to top: Blue line: original PBS; orange line: original PPeF; grey line: original PBS/PPeF physical blend; yellow line: original P(BS-*b*-PeF)$_{15}$ copolymer; light blue line: P(BS-*b*-PeF)$_{15}$ after 9 h hydrolysis with 1 µM HiC. Main peaks for discussion are indicated in the spectrum with black (hydrolysis related peak), orange: PPeF uniquely assigned main peaks, blue: PBS uniquely assigned peaks. B: FT-IR stacked spectra of P(BS-*b*-PeF)$_{15}$ copolymer before and after incubation with 1 µM HiC 9 h.

copolymer, thus the enzyme showed preferentiality to specific portions of the surface.

The surface of the partially hydrolysed samples was also characterized through FT-IR to differentiate the sequential removal of each component from the blend and copolymer. Fig. 4A superimposes the original samples with the treated copolymer with the lowest concentration of enzyme after 9 h of incubation with a zoom in the region 650 cm^{-1} – 1850 cm^{-1}(full spectra available in Figure S6, ESI). Containing the most intense peaks, this region highlights the main differences, which related to the surface of the polymers.

The 1485 cm^{-1} area showed unique peaks for PBS, relatable to the symmetric deformational vibrations of -CH_2- groups in its main chain. As a result, the physical blend and the copolymer displayed a unique large peak in this region, while a medium intense peak (O—C-O stretching) could be located at 1050 cm^{-1} for PBS and at 1020 cm^{-1} for PPeF, resulting in another double peak in the blend and in the copolymer. While in fact, the physical blend surface showed a prevalence for the PBS peak, the opposite was observed in the copolymer, where PPeF band appeared similarly intense. The same was recorded in the range 950–970 cm^{-1} (-C-OH bending of PBS carboxylic groups) and 800–825 cm^{-1}. 1385 cm^{-1}, 1330 cm^{-1} and 1315 cm^{-1} bands presented double peaks configuration in PBS containing samples, but not in PPeF homopolymer. The residual copolymer after incubation showed still a high similarity to the original sample. Nevertheless, the peaks that were exclusively attributable to PBS appeared less intense in relative terms.

The peak located around 1700 cm^{-1} was distinguishable into three main bands: 1712 cm^{-1}, 1720 cm^{-1} and 1733 cm^{-1}, undergoing a change in shape throughout the incubation (Fig. 4B) The band at 1712 cm^{-1} is associated to aryl ester stretching of the aromatic monomer, FDCA (from PPeF) and its intensity reduction in the treated samples, also in the copolymer after 9 h incubation, is a clear sign of hydrolysis. The second band, 1720 cm^{-1}, relates instead to the double bond stretching of the carbonyl =CO, while the third, 1733 cm^{-1}, associates to the aliphatic ester stretching. The latter in particular also decreases in intensity, consistently to what previously reported [26].

Oppositely, 1580 cm^{-1}, 1385 cm^{-1}, 986 cm^{-1} and 762 cm^{-1} are additional wavelengths in which PPeF uniquely associated peaks were located, suggesting their use as a reference to track PPeF hydrolysis in the blend/copolymer. 986 cm^{-1} and 762 cm^{-1} were associated with =CH out of plane bending of disubstituted furan ring, absent in PBS. In addition, PPeF main ester peak showed a shoulder at around 1300 cm^{-1}, which could not be identified in PBS spectrum. Other strong peaks appeared shifted in the PBS profile: 1125 cm^{-1} shifted of circa 25 cm^{-1} compared to PPeF spectrum. This was particularly visible in the copolymer spectra since this area resulted as a double peak. They are both nonetheless attributable to -C-O—C ester group, but the shift could be explained by the specific surrounding chemical environments to which they react. The signal located at around 762 cm^{-1}, related to the vibration of the furan ring namely, did not change between the original copolymer and the treated sample, showing that the furan domain underwent minor changes. These data corroborate weight loss and monomer quantifications, where PBS resulted the most readily hydrolysed component (singular spectra are available at Figure S7–8, ESI).

The region between 3100 and 2800 cm^{-1} included peaks relatable to both PPeF -COOH and =CH groups of the furan ring stretches and PBS -COOH vibration and asymmetric stretching vibration of -CH_2- group, which is common among all polyesters [27] (Figure S6).

3.4. ^{1}H NMR analysis of the lyophilized hydrolysate

The obtained hydrolysate was used for molecular investigation using ^{1}H NMR spectroscopy. The samples were lyophilized to remove all water, resolubilized in deuterated chloroform and filtered through cotton to obtain a clear solution from which all insoluble salts were removed. Since the whole sample was solubilized and analysed, it was possible to have a comprehensive overview of the species present in the mixture. Nonetheless, some of the monomers (e.g. 1,4-butanediol and succinic acid) proved not to be completely soluble in chloroform, but the unequivocal assignment to the residual chemical groups from the polymer was anyhow possible. The integrated area of the peaks was used as a quantification of the intensity, therefore as an indicator of the relative abundance of the associated chemical group.

In particular, 7.2 ppm resonance was associated to the FDCA ring protons, while 1,5-pentanediol methylene groups and esterified -CH_2- protons of PPeF (C–O–C$\underline{H_2}$CH_2CH_2–) shifted at 1.5, 1.8 and 4.3 ppm respectively (indicated as F/E and D, in Fig. 5). PBS alpha-methylene and beta-methylene in 1,4-butanediol were associated to 4.1 and 1.7 ppm signals (A and B in Fig. 5), while succinic acid beta-methylene protons could be traced at 2.6 ppm (C in Fig. 5). The three groups (A, B and C) from PBS stand at 1:1:1 ratio, for direct comparison. A and D signals decreased progressively with increased incubation time. Since they correspond to both polymers esterified C—O-CH_2- protons, their intensity could be referred to evaluate the hydrolysis of the ester bonds by means of the cutinase. In fact, the integrated area at these peaks declined more significantly in the enzymatically treated samples, compared to the slightly inferior intensity in the control sample after 24 h.

Signals between 3.4 ppm and 3.7 ppm were instead attributable to the terminal -CH_2—C$\underline{H_2}$—OH group, therefore the not esterified endings of the diols (H in Fig. 5). They are not present in the original or control samples. Their presence in the treated samples, with an increasing intensity in the longer incubation samples, constituted a further confirmation of the occurred hydrolysis.

The PBS/PPeF physical blend was also analysed via ^{1}H NMR but no significant differences among samples were observed due to the very fast hydrolysis reaction of the polymer (Figure S9, ESI).

3.5. Gel permeation chromatography of the hydrolysates

The adopted settings for HPLC allowed the quantification of the released soluble monomers in the hydrolysate. The depolymerization mechanism was further characterized through GPC analysis on the residual polymers after enzymatic hydrolysis. For this analysis, samples were solubilized in chloroform at a final concentration of ~2 mg mL^{-1}. PBS and PPeF shows both M and Mw higher than PPeF, suggesting that at the beginning of the incubation, the polymer chains are longer and the molecular weight distribution is wider. As it can be seen from Fig. 6, already after 3 h of reaction there was a complete conversion of PBS into its constituent monomers with $a > 99$ % decrease of the observed molecular weight of the polymer. This fast hydrolysis reaction of PBS was somehow expected as it is an aliphatic polyester like cutin, the natural substrate of cutinases [28]. On the contrary, a lower decrease in the molecular weight was seen for PPeF (Fig. 6) indicating a slower enzymatic hydrolysis of ester bonds between furan ring and 1,5-pentamethylene segment. Despite the slower depolymerization, a complete conversion to monomers was observed after 24 h of reaction. In fact, PPeF Mn decreases within the first time point, reversing the trend between 3 and 9 h, indicating a possible polymer rearrangement before the final degradation by 24 h. As seen for weight loss and released monomers, GPC analysis likewise indicated faster depolymerisation of the PBS/PPeF physical blend when compared to the copolymer (Fig. 6 grey vs yellow bars), although the difference between the blend and copolymer seen regarding molecular weight decreases (Mn) within the first phase was even more pronounced then based on weight loss and release of monomers. The GPC results confirm the faster enzyme attack towards the aliphatic semicrystalline PBS with respect to the aromatic amorphous PPeF. When combined, PPeF fraction, especially if chemically linked, hinders the hydrolysis PBS segments. Mw and Mn raw data are reported in Table S3 (ESI). Mw aligns with Mn trends, as PBS and the physical blends Mw values decrease more drastically within the first time point, compared to PPeF and the copolymer Mw. However, Mw is initially larger than Mn for the four polymers, indicating a higher

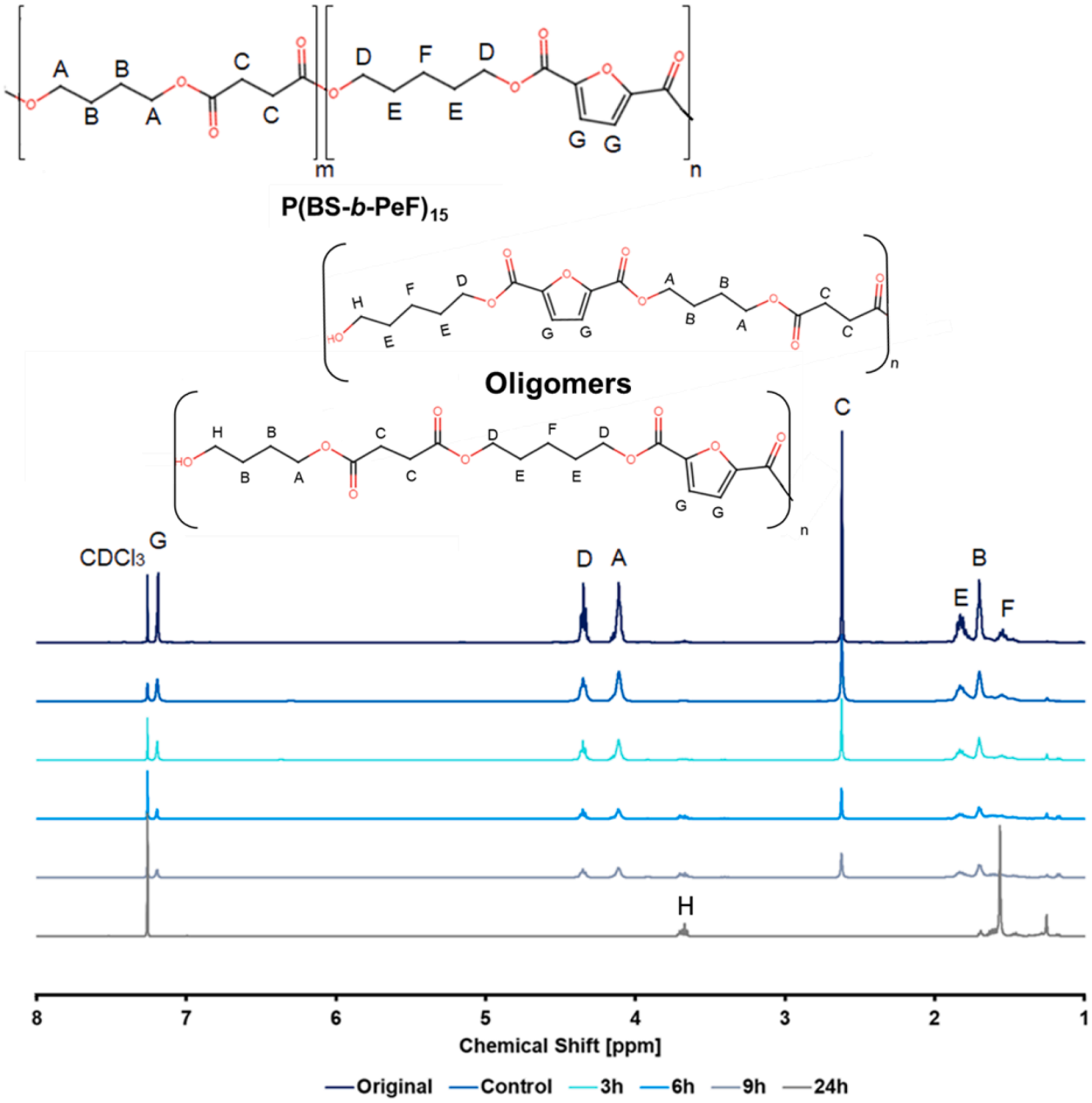

Fig. 5. ^{1}H NMR spectra of the PBS/PPeF based copolymer hydrolysed 1 μM HiC, lyophilized and then solubilized in $CDCl_3$ and plotted according to the time points. Assignments to the molecule chemical groups are reported with letters present in the reference structure.

dispersity of polymer chain lengths (up to higher molecular weight chains). In the course of degradation, the ratio between Mw and Mn decreases, consistently with the polymer breaking down into smaller fragments, although Mw stays higher than Mn, implying that after hydrolysis, longer molecules still persist. It is worth noting that although the polymer initial molecular weight influences degradation rate, as shorter chains corresponds to higher enzyme accessibility, the enzymatic degradation is the result of the interplay of several factors in addition. Crystallinity, phases, miscibility and composition, as already discussed, altogether contribute to the different degradation behaviour.

4. Conclusion

Blending and synthesis of copolymers provides a versatile tool to combine the advantages of each individual component and create improved products. Nevertheless, each new formulation can display a different mechanical/chemical behaviour as well as a distinctive biodegradation mechanism compared to the single units. Therefore, it is necessary to assess depolymerization performance, especially in the perspective of a total green management of new competitive environmentally friendly polymers, as furans with the increasing variety of their class.

As demonstrated previously, PPeF blended with PLA resulted in polymers, whose PPeF component is removed from enzymes in shorter incubation time than the PLA present in the same formulation. Opposite results were observed for the combination of PPeF with PBS. In general, PBS and PPeF homopolymers, as well as their equiponderal physical blend and block copolymer, proved to be 100 % enzymatically degradable in the applied system (in terms of weight loss, which ratifies an additional advantage for these formulations. Complete weight loss was recorded for all the samples within 24 h, which allowed the decrease of incubation time from 24 h to 9 h and the concentration of enzyme

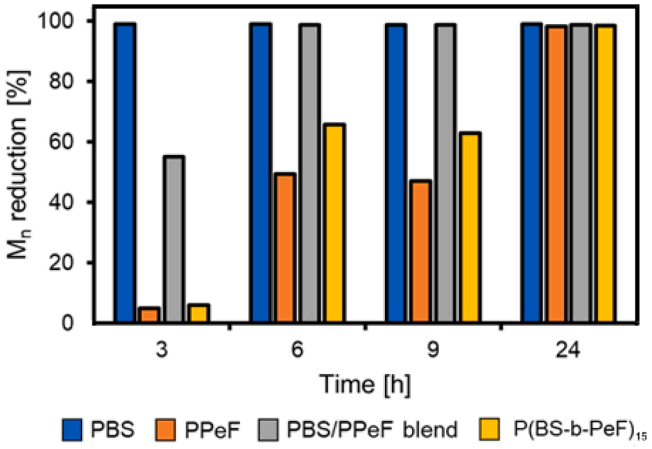

Fig. 6. Gel permeation analysis of pure PBS and PPeF and their blend and copolymer. The y axis shows the reduction of the number average molecular weight (M_n) of the polymers at the various considered time points when compared with the starting material before hydrolysis. Blue bars: PBS; orange bars: PPeF; grey bars: PBS/PPeF blend; yellow bars: P(BS-*b*-PeF)$_{15}$.

from 5 μM to 1 μM. ^{1}H NMR and GPC analysis of the hydrolysates further confirm the easy enzymatic depolymerization of PBS and that its combination with PPeF resulted in slower hydrolysis rates with the physical blend getting depolymerized faster than the covalently linked P(BS-*b*-PeF) copolymer. This indicates that intrinsic enzyme-based recycling properties could be adjusted during development of novel polymers. Likewise, biodegradation could be tuned since in nature extracellular enzymes are responsible for the first step of polymer decomposition before monomers can be taken up by microbial cells.

This work poses the basis for deep investigations of the relationship between polymer structures and enzymatic degradability, given the growing availability of biobased blends for packaging. A broader family of copolymers with different sequences of blocks needs to be researched to explore whether the copolymer designs reduce degradability *per se* or could be further carefully customized. In addition to different enzyme concentration, environmental conditions such as pH and temperature, will be also valuable to be investigated to determine the applicability of these polymers in diverse settings.

CRediT authorship contribution statement

Chiara Siracusa: Writing – original draft, Methodology, Investigation, Formal analysis. **Mattia Manfroni:** Visualization, Methodology, Investigation. **Alessandro Coatti:** Visualization, Methodology, Investigation. **Felice Quartinello:** Writing – review & editing, Visualization, Validation, Supervision. **Michelina Soccio:** Writing – review & editing, Validation, Supervision, Resources, Project administration, Data curation, Conceptualization. **Nadia Lotti:** Writing – review & editing, Validation, Supervision, Resources, Project administration, Funding acquisition. **Georg M. Guebitz:** Writing – review & editing, Supervision, Resources, Project administration, Funding acquisition. **Alessandro Pellis:** Writing – review & editing, Validation, Supervision, Resources, Project administration, Funding acquisition, Conceptualization.

Declaration of competing interest

The authors declare that they have no known competing financial interests or personal relationships that could have appeared to influence the work reported in this paper.

Acknowledgements

This research was funded by the European Union's Horizon 2020 research and innovation program under grant agreement No 953073 and the project UPLIFT (sUstainable PLastIcs for the Food and drink packaging indusTry).

Supplementary materials

Supplementary material associated with this article can be found, in the online version, at doi:10.1016/j.polymdegradstab.2025.111631.

Data availability

The data supporting this article have been included as part of the Supplementary Information.

References

[1] Eurostat, EU packaging waste generation with record increase. 2023 Accessed: Jun. 05, 2024 [Online]. Available: https://ec.europa.eu/eurostat/web/products-eurostat-news/w/ddn202310191#:~:text=From%20parcels%20for%20online%20purchases,kg%20more%20than%20in%202011.

[2] European Parliament, Packaging: new EU rules to reduce, reuse and recycle. 2023 Accessed: Jun. 05, 2024. [Online]. Available: https://www.europarl.europa.eu/news/en/press-room/20231023IPR08128/packaging-new-eu-rules-to-reduce-reuse-and-recycle.

[3] European Parliament and Council, European Parliament and Council Directive 94/62/EC of 20 December 1994 on packaging and packaging waste [Online]. Available, https://eur-lex.europa.eu/legal-content/EN/TXT/?uri=celex%3A31994L0062, 1994.

[4] A.F. Sousa, et al., Biobased polyesters and other polymers from 2,5-furandicarboxylic acid: a tribute to furan excellency, Polym. Chem. 6 (33) (2015) 5961–5983, https://doi.org/10.1039/c5py00686d.

[5] V. Tsanaktsis, Z. Terzopoulou, M. Nerantzaki, G.Z. Papageorgiou, D.N. Bikiaris, New poly(pentylene furanoate) and poly(heptylene furanoate) sustainable polyesters from diols with odd methylene groups, Mater. Lett. 178 (2016) 64–67, https://doi.org/10.1016/j.matlet.2016.04.183.

[6] G. Guidotti, et al., Fully biobased superpolymers of 2,5-furandicarboxylic acid with different functional properties: from rigid to flexible, high performant packaging materials, ACS Sustain. Chem. Eng. 8 (25) (2020) 9558–9568, https://doi.org/10.1021/acssuschemeng.0c02840.

[7] M. Jiang, Q. Liu, Q. Zhang, C. Ye, G. Zhou, A series of furan-aromatic polyesters synthesized via direct esterification method based on renewable resources, J. Polym. Sci. Part A Polym. Chem. 50 (5) (2012) 1026–1036, https://doi.org/10.1002/pola.25859.

[8] V. Tsanaktsis, G.Z. Papageorgiou, D.N. Bikiaris, A facile method to synthesize high-molecular-weight biobased polyesters from 2,5-furandicarboxylic acid and long-chain diols, J. Polym. Sci. Part A Polym. Chem. 53 (22) (2015) 2617–2632, https://doi.org/10.1002/pola.27730.

[9] A. Little, et al., Effects of methyl branching on the properties and performance of furandioate-adipate copolyesters of bio-based secondary diols, ACS Sustain. Chem. Eng. 8 (38) (2020) 14471–14483, https://doi.org/10.1021/acssuschemeng.0c04513.

[10] M.R. Miah, Y. Dong, J. Wang, J. Zhu, Recent progress on sustainable 2,5-furandicarboxylate-based polyesters: properties and applications, ACS Sustain. Chem. Eng. 12 (8) (2024) 2927–2961, https://doi.org/10.1021/acssuschemeng.3c06878.

[11] S. Weinberger, et al., Enzymatic surface hydrolysis of poly(ethylene furanoate) thin films of various crystallinities, Green Chem 19 (22) (2017) 5381–5384, https://doi.org/10.1039/c7gc02905e.

[12] European bioplastics, Bioplastics Market Development Update 2023, 2023, December 2023, pp. 2022–2023 [Online]. Available, https://docs.european-bioplastics.org/publications/market_data/2023/EUBP_Market_Data_Report_2023.pdf.

[13] V. Siracusa, N. Lotti, A. Munari, M.Dalla Rosa, Poly(butylene succinate) and poly (butylene succinate-co-adipate) for food packaging applications: gas barrier properties after stressed treatments, Polym. Degrad. Stab. 119 (2015) 35–45, https://doi.org/10.1016/j.polymdegradstab.2015.04.026.

[14] M. Gigli, M. Fabbri, N. Lotti, R. Gamberini, B. Rimini, A. Munari, Poly(butylene succinate)-based polyesters for biomedical applications: a review in memory of our beloved colleague and friend Dr. Lara Finelli, Eur. Polym. J. 75 (2016) 431–460, https://doi.org/10.1016/j.eurpolymj.2016.01.016.

[15] O. Platnieks, S. Gaidukovs, V. Kumar Thakur, A. Barkane, S. Beluns, Bio-based poly (butylene succinate): recent progress, challenges and future opportunities, Eur. Polym. J. 161 (October) (2021) 110855, https://doi.org/10.1016/j.eurpolymj.2021.110855.

[16] L. Aliotta, M. Seggiani, A. Lazzeri, V. Gigante, P. Cinelli, A brief review of Poly (Butylene Succinate) (PBS) and its main and applications, Polymer (Guildf) 14 (2022) 844.

[17] N. Kantor-Malujdy, S. Skowron, B. Michalkiewicz, M. El Fray, Poly(butylene-succinate)-based blends with enhanced oxygen permeability, Mater. Today Commun. 33 (August) (2022) 104306, https://doi.org/10.1016/j.mtcomm.2022.104306.

[18] A.F. Sousa, et al., Recommendations for replacing PET on packaging, fiber, and film materials with biobased counterparts, Green Chem 23 (22) (2021) 8795–8820, https://doi.org/10.1039/d1gc02082j.
[19] N. Manfroni, M. Coatti, A. Soccio, M. Siracusa, V. Boanini, E. Salatelli, E. Lotti, Eco-design of biobased poly(butylene succinate-b-pentamethylene 2,5-furanoate) copolymers with optimized mechanical, thermal and barrier properties for flexible food-packaging, Eur. Polym. J. 225 (2025) 113728, https://doi.org/10.1016/j.eurpolymj.2025.113728.
[20] G. Guidotti, et al., Evidence of a 2D-ordered structure in biobased poly (pentamethylene furanoate) responsible for its outstanding barrier and mechanical properties, ACS Sustain. Chem. Eng. 7 (21) (2019) 17863–17871, https://doi.org/10.1021/acssuschemeng.9b04407.
[21] W. Pan, Z. Bai, T. Su, Z. Wang, Enzymatic degradation of poly(butylene succinate) with different molecular weights by cutinase, Int. J. Biol. Macromol. 111 (2018) 1040–1046, https://doi.org/10.1016/j.ijbiomac.2018.01.107.
[22] S. Weinberger, et al., Enzymatic degradation of poly(Ethylene 2,5-furanoate) powders and amorphous films, Catalysts 7 (11) (Nov. 2017), https://doi.org/10.3390/catal7110318.
[23] C. Siracusa, et al., On the selective enzymatic recycling of poly(pentamethylene 2,5-furanoate)/poly(lactic acid) blends and multiblock copolymers, ACS Sustain. Chem. Eng. 11 (26) (2023) 9751–9760, https://doi.org/10.1021/acssuschemeng.3c01796.
[24] S. Su, R. Kopitzky, S. Tolga, S. Kabasci, Polylactide (PLA) and its blends with poly (butylene succinate) (PBS): a brief review, Polymers (Basel) 11 (7) (2019) 1–21, https://doi.org/10.3390/polym11071193.
[25] H.P. Austin, et al., Characterization and engineering of a plastic-degrading aromatic polyesterase, Proc. Natl. Acad. Sci. U. S. A. 115 (19) (2018) E4350–E4357, https://doi.org/10.1073/pnas.1718804115.
[26] Y.J. Phua, W.S. Chow, Z.A. Mohd Ishak, Reactive processing of maleic anhydride-grafted poly(butylene succinate) and the compatibilizing effect on poly(butylene succinate) nanocomposites, Express Polym. Lett. 7 (4) (2013) 340–354, https://doi.org/10.3144/expresspolymlett.2013.31.
[27] M.A. Tadda, et al., Impacts of Baobab (Adansonia digitata) powder on the poly (Butylene Succinate) polymer degradability to form an eco-friendly filler-based composite, Front. Mater. 8 (November) (2021) 1–10, https://doi.org/10.3389/fmats.2021.768960.
[28] S. Ibrahim, O. Riahi, S.M. Said, M.F.M. Sabri, S. Rozali, Biopolymers from crop plants, Ref. Modul. Mater. Sci. Mater. Eng. (2019) 1–10, https://doi.org/10.1016/b978-0-12-803581-8.11573-5.